JOURNAL OF AGRICULTURAL AND FOOD CHEMISTRY

pubs.acs.org/JAFC

Article

Inhibition of the Occurrence and Development of Inflammation-Related Colorectal Cancer by Fucoidan Extracted from *Sargassum fusiforme*

Xiang Li,[⊥] Shijun Xin,[⊥] Xiaoqun Zheng,[⊥] Liqin Lou, Shiqing Ye, Shengkai Li, Qilong Wu, Qingyong Ding, Ling Ji, Chunrong Nan, and Yongliang Lou*

Cite This: *J. Agric. Food Chem.* 2022, 70, 9463−9476

Read Online

ACCESS | Metrics & More | Article Recommendations

ABSTRACT: Fucoidan has many biological activities, including the inhibitory effect on the development of various cancer types. This study showed that lipopolysaccharide-induced inflammation in FHC cells (normal human colonic epithelial cells) could be reversed using fucoidan at different concentrations. The fucoidan-induced anti-inflammatory effect was also confirmed through *in vivo* experiments in mice. Compared to the mice of the model group, the ratio of Firmicutes/Bacteroidetes in feces increased and the diversity of gut microbial composition was restored in mice after fucoidan intervention. In colorectal cancer (CRC) cells DLD-1 and SW480, fucoidan inhibited cell proliferation and promoted cell apoptosis. It also blocked the cell cycle of DLD-1 and SW480 at the G0/G1 phase. The animal model of inflammation-related CRC showed that the incidence of tumors in mice was significantly reduced by fucoidan intervention. Furthermore, the administration of fucoidan decreased the expression levels of inflammatory factors such as TNF-α IL-6 and IL-1β in the colonic tissues. Therefore, fucoidan can effectively prevent the development of colitis-associated CRC.

KEYWORDS: *fucoidan, colorectal cancer, colitis, intestinal microecology*

INTRODUCTION

The International Agency for Research on Cancer (IARC) has shown that colorectal cancer (CRC) has the third-highest incidence and the second-highest mortality among all cancer types worldwide in 2020.[1] In fact, it accounted for 10% of newly diagnosed cancer cases and 9.4% cancer-related deaths worldwide in 2020, making it the second most common cancer of the year. The CRC has complex causes, including factors such as genetics, diet, and inflammation.[2,3] Despite the increasing diversity of clinical approaches for the treatment of tumors,[4,5] the prognosis of patients with CRC remains unsatisfactory. Therefore, novel therapeutic approaches need to be developed urgently for improving the prognosis of patients with CRC.[6]

Currently, inflammatory bowel disease-associated colorectal cancer (IBD-CRC) is recognized as the most severe condition that can give rise to IBD-related complications.[7] Many reports have suggested that prolonged intestinal inflammation greatly increases the risk of developing CRC.[8,9] Patients with inflammation-associated CRC tend to have worse outcomes.[10] Progression from colitis to CRC is a continuous dynamic process and is often accompanied by dysbiosis and a compromised gut barrier.[11,12]

The intestinal microflora is a highly complicated community comprising mainly of bacteria, viruses, fungi, and archaea.[13] The rich and diverse intestinal microbes maintain our health in a dynamic balance. As the intestine is the most dominant organ inhabited by human flora, the development of several enteropathies is inextricably linked to microorganisms.[14] There is growing evidence that a dysbiosis of the intestinal microflora can trigger and promote diseases mediated by chronic inflammation, including CRC.[15−17] *Bacteroides fragilis* and *Fusobacterium nucleatum* are the key bacteria responsible for colorectal carcinogenesis.[18] In patients with CRC, the ratio of Firmicutes/Bacteroidetes in the stool is significantly higher than that of controls.[19] In addition, the bacterial metabolites, including short-chain fatty acids, are essential for protecting the gut mucosal barrier and inhibiting intestinal inflammation.[20]

Sargassum fusiforme is perennial temperate seaweed and is mainly found in the southeast coast of China, the Yellow Sea, as well as the neighboring waters. It belongs to the class of brown seaweed (Phaeophyceae) and has unique nutritional and medicinal values.[21] It is a major source of dietary fibers and polysaccharides, including fucoidan, alginic acid, and laminaran.[21] Fucoidan is a type of sulfated polysaccharide that is mainly extracted from marine brown algae. It is the most potent pharmacological component of seaweed such as *S. fusiforme*.[22] Fucoidan is noncytotoxic to normal cell lines such as 293T and FHC (normal human colonic epithelial cells);[23,24] however, it is cytotoxic to various cancer cells because it inhibits their

Received: April 5, 2022
Revised: July 8, 2022
Accepted: July 8, 2022
Published: July 20, 2022

https://doi.org/10.1021/acs.jafc.2c02357
J. Agric. Food Chem. 2022, 70, 9463−9476

proliferation and blocks their cell cycles.[25] In addition, fucoidan is involved in stabilizing the composition of the microbial community in the gut of mice.[26] However, not much is known about the mechanism through which fucoidan inhibits the proliferation of cancerous cells. At present, only a few studies have explored the function and role of fucoidan obtained from *S. fusiforme* in cancer.[27,28] In addition, no studies so far have investigated the effect of fucoidan extracted from *S. fusiforme* on CRC. This study is an attempt to fill in this gap.

MATERIALS AND METHODS

Fucoidan Preparation. After reflux treatment with 90% ethanol, the *S. fusiforme* powder was dissolved with water at 70 °C for 2 h (material to water ratio of 1:10). The filter residue was extracted by centrifugation at 3000 rpm for 15 min. The above steps were performed twice. All of the supernatant was collected and filtered. The filtrate was filtered and washed with ethanol to a concentration of 75% after ultrafiltration and then freeze-dried. The dried powder was dissolved into a 2% aqueous solution. Next, HCl was added to achieve a solution of pH 2.0. The filtrate was neutralized with alkali and ethanol was added to 75%. The resulting precipitate was dissolved with acetone and ethanol after filtration and then dried at 40 °C to obtain fucoidan. The total fucoidan assay of the sample was 98.1% fucoidan, with 22% of L-fucose. Barium sulfate turbidimetric analysis revealed the presence of 22.8% of organic sulfates in the fucoidan sample.

Animal Studies. Male BALB/c mice with an age of 6−8 weeks (Beijing Vital River Laboratory Animal Technology Co., Ltd.) were fed at the experimental animal center of Wenzhou Medical University. All animal studies were conducted in compliance with the animal experiment guidelines of Wenzhou Medical University. The protocols were approved by the Animal Experimental Ethics Committee (wydw2019-0944).

The animals were divided into three groups by randomization, with six mice in each group. The mice used in the colitis experiment were fed adaptively for a week. Mice in the model group and the treatment group were fed with 4% dextran sulfate sodium salt (DSS, w/v; Aladdin, Shanghai, China) for 7 days. The treatment group was additionally treated with fucoidan at 1 g kg^{-1} per day. The weight, episodes of diarrhea, bloody stool, and other conditions of the mice were recorded every day. Table 1 shows the criteria of the disease activity index (DAI) score.[29] After adaptation, mice in both the model and treatment groups were administered with azoxymethane (AOM; 12 mg kg^{-1}; Sigma) through intraperitoneal injection. On the 8th day after AOM injection, the model and treatment groups were fed with 2.5% DSS for 7 days and then given normal water for the next 7 days, in a cycle of three. Mice in the control group were provided with normal water throughout the experiment. After 12 weeks, the mice were euthanized and weighed, and their appearance was noted. The tumor-bearing colorectal tissues of the mice were fixed with 4% paraformaldehyde. The remaining colorectal tissues and cecal contents were preserved at −80 °C.

Table 1. Disease Activity Index (DIA) Score Standard

weight loss (%)	stool consistency	visible blood in feces	score
none	normal stool	none	0
1−5			1
6−10	loose stool	slightly bleeding	2
10−20			3
>20	diarrhea	gross bleeding	4

Cell Culture. The FHC, SW480, and DLD-1 cell lines were purchased from ATCC. The FHC cells were cultured in the RPMI-1640 medium, and the SW480 and DLD-1 cells were cultured in the Dulbecco's Modified Eagle Medium (DMEM) in an incubator with 5% CO_2 at 37 °C. Penicillin G (100 U mL^{-1}), streptomycin (100 mg mL^{-1}) (Beyotime, Nanjing, China), and 10% FBS (Invitrogen, Waltham, MA) were added to the culture medium.

Cell Viability. The cultured cells were digested and seeded in a 96-well plate at a concentration of 8000 cells/well and maintained overnight in a cell incubator. Next, the medium containing different concentrations of fucoidan replaced the original media. After 24 h, the cells were incubated with 10 μL of 3-(4,5-dimethyl-2-thiazolyl)-2,5-diphenyl-2-H-tetrazolium bromide (MTT) (5 mg mL^{-1}) at 37 °C in the presence of 5% CO_2 for 4 h. Then, the cells were dissolved in a solution of dimethyl sulfoxide (DMSO; Sigma-Aldrich). A plate reader (BioTek Instruments, Winooski, VT) was used to analyze the cell viability at a wavelength of 570 nm.

Colony-Formation Assay. A single-cell suspension of SW480 and DLD-1 cells was prepared. This suspension was evenly inoculated into six-well plates at a density of 800 cells/well and then cultured in a cell incubator. The cells were fixed using 4% paraformaldehyde (Solarbio, Beijing, China) for 30 min. Then, the cells were stained with crystal violet (Beyotime, Nanjing, China) for another 30 min, washed with sterile water, and then dried in air. The number of cell clones formed was counted manually.

Cell Apoptosis Analysis. The cultured cells were incubated with fucoidan and then harvested and resuspended with 1× binding buffer. Next, they were dyed with 10 μL of 7-AAD and 5 μL of AnnexinV-PE and incubated in the dark for 5 min at room temperature. Flow cytometry was used to perform cell apoptosis analysis. Finally, the apoptosis rate was evaluated by Flow J software.

Cell Cycle Analysis. Cells treated with fucoidan at different concentrations were resuspended with 500 μL of 1× RNase A solution. Next, 5 μL of PI was added. 1× RNase A solution and PI were mixed and the cells were stained for 30 min in the dark. Flow cytometry and CytExpert were used for cell cycle analysis.

Western Blot. Bicinchoninic acid (BCA) protein assay was conducted to analyze the total protein concentrations. After sodium dodecyl sulfate polyacrylamide gel electrophoresis, the samples were transferred to the poly(vinylidene difluoride) membranes. Skim milk was used for incubation with specific primary antibodies (1:1000 dilution) at 4 °C overnight. The antibodies included cleaved-caspase3 (Diagbio, Hangzhou, China), cleaved-PARP (Diagbio, Hangzhou, China), Cdk2 (Diagbio, Hangzhou, China), Cyt-c (Diagbio, Hangzhou, China), p21 (Diagbio, Hangzhou, China), cyclinE1 (Huabio, Hangzhou, China), total STAT3 (t-STAT3; Diagbio, Hangzhou, China), phosphorylated STAT3 (p-STAT3; Diagbio, Hangzhou, China), β-actin (Abways, Beijing, China), and GAPDH (Abways, Beijing, China). The samples were incubated with secondary antibodies (1:2000 dilution) (Biosharp) at a constant room temperature. The bands of protein were visualized using a hypersensitive enhanced chemiluminescence kit (Beyotime, Nanjing, China). The Bio-Rad gel imaging system was photographed, and ImageJ software was used for system analysis.

RT-qPCR. Trizol was used for the extraction of total RNA. cDNA was generated by reverse transcription. The prepared polymerase chain reaction (PCR) solution and cDNA were placed in PCR 8-strip tubes for conducting RT-qPCR. The primer sequences are shown in Tables 2 and 3. The reaction conditions were as follows: Stage 1: 95 °C for 30 s, once; Stage 2: 95 °C for 5 s, 60 °C for 60 s, with a total of 40 cycles; and Stage 3: Dissociation.

Table 2. Prime Sequence (Cell)

prime name (cell)	prime sequence
TNF-α	F:5′-ATGTTGTAGCAAACCCTCAAGC-3′
	R:5′-TGTGGGTGAGGAGCACAT-3′
IL-6	F:5′-CAATGAGGAGACTTGCCTGGTG-3′
	R:5′-GGTTGGGTCAGGGGTGGTTA-3′
IL-1β	F:5′-CAACAGGCTGCTCTGGGATT-3′
	R:5′-GTCCTGGAAGGAGCACTTCAT-3′
IL-8	F:5′-TTGCCAAGGAGTGCTAAAGAA-3′
	R:5′-GCCCTCTTCAAAAACTTCTCC-3′
GAPDH	F:5′-TGGACTCCACGACGTACTCAG-3′
	R:5′-ACATGTTCCAATATGATTCCA-3′

https://doi.org/10.1021/acs.jafc.2c02357
J. Agric. Food Chem. 2022, 70, 9463−9476

Table 3. Prime Sequence (Animal)

prime name (animal)	prime sequence
TNF-α	F:5′-CTCCAGGCGGTGCCTATG-3′
	R:5′-GGGCCATAGAACTGATGAGAGG-3′
IL-6	F:5′-GCTACCAAACTGGATATAATCAGGA-3′
	R:5′-CCAGGTAGCTATGGTACTCCTGAA-3′
IL-1β	F:5′-TCACAGCAGCACATCAACAA-3′
	R:5′-TGTCCTCATCCTGGAAGGT-3′
iNOS	F:5′-CACCAAGCTGAACTTGAGCG-3′
	R:5′-CGTGGCTTTGGGCTCCTC-3′
β-actin	F:5′-GGCTGTATTCCCCTCCATCG-3′
	R:5′-CCAGTTGGTAACAATGCCATGT-3′

ELISA. First, 10 mg of the colonic tissues of mice was ground with 100 μL of PBS. The supernatant was retained. The IL-6, TNF-α, IL-1β, and iNOS levels were detected by ELISA kits (qzkndbio, Quanzhou, China). The instructions were strictly followed.

Histologic Analysis. The colorectal tissues were first fixed in 4% paraformaldehyde for 24 h and then embedded in the paraffin. The wax blocks were cut into 5-μm-thick slices, which were then stained with eosin and hematoxylin (Beyotime, Nanjing, China). The general morphological changes were observed under the microscope. The content of mucin was evaluated under the microscope by staining with nuclear fast red and Alcian blue (pH 2.5) (Beyotime, Nanjing, China).

16S rDNA Sequencing. The total genomic DNA of mice was obtained from their cecal contents. The genes of 16S/18S rRNA were amplified using the specific primer with the barcode. All PCRs steps were conducted in the reaction media (30 μL) containing 15 μL of High-Fidelity PCR Master Mix (New England Biolabs). The following thermocycling conditions were used: predegeneration at 98 °C for 1

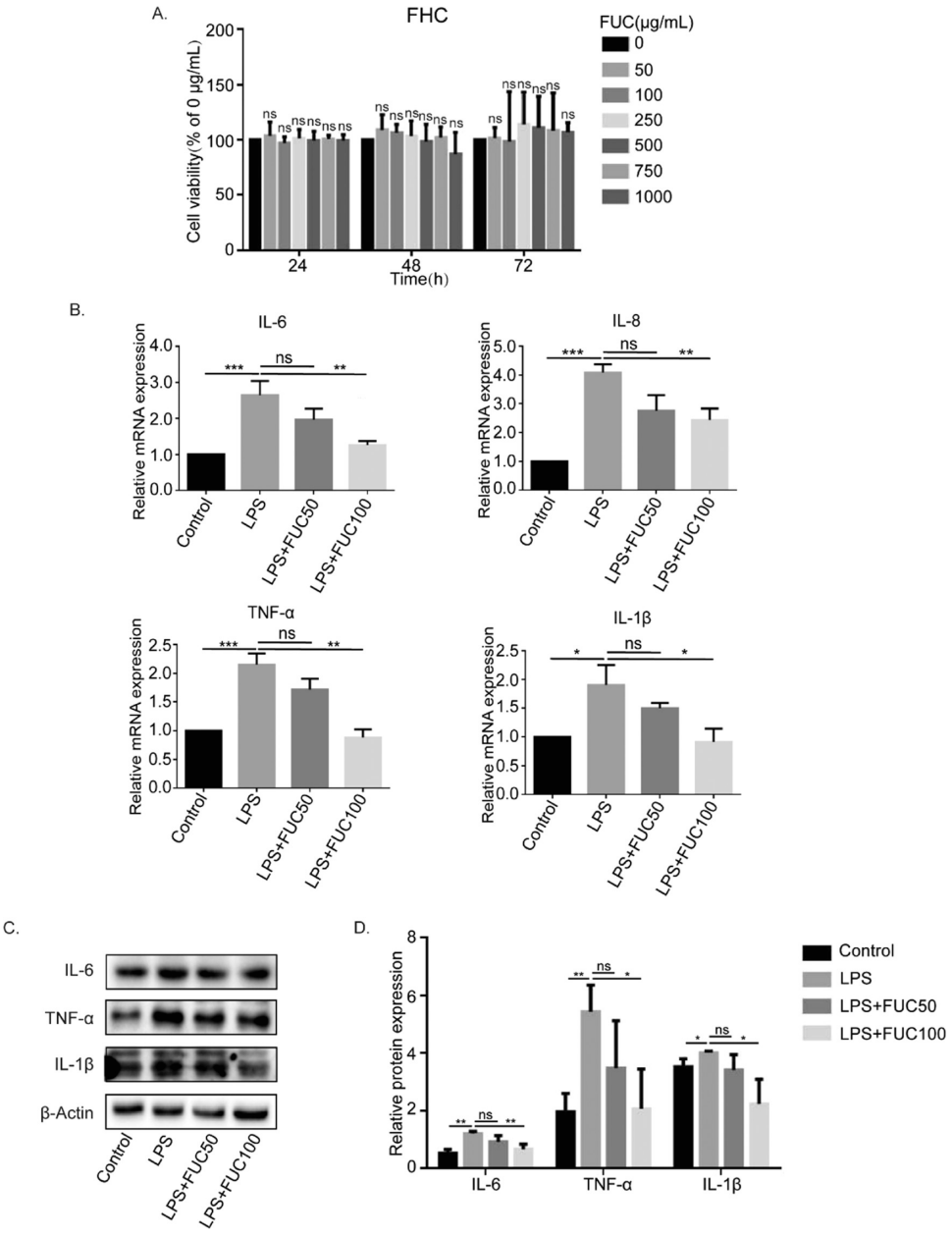

Figure 1. Fucoidan is not cytotoxic to FHC cells and relieves LPS-induced inflammation of FHC cells. (A) MTT results after fucoidan treatment of FHC. (B) RT-qPCR results of inflammatory factors after treatment with LPS-induced FHC by fucoidan. (C, D) WB results and statistical analysis of inflammatory factors after treatment with LPS-induced FHC by fucoidan. *P < 0.05, **P < 0.01, ***P < 0.001, ns P > 0.05 vs Control.

https://doi.org/10.1021/acs.jafc.2c02357
J. Agric. Food Chem. 2022, 70, 9463−9476

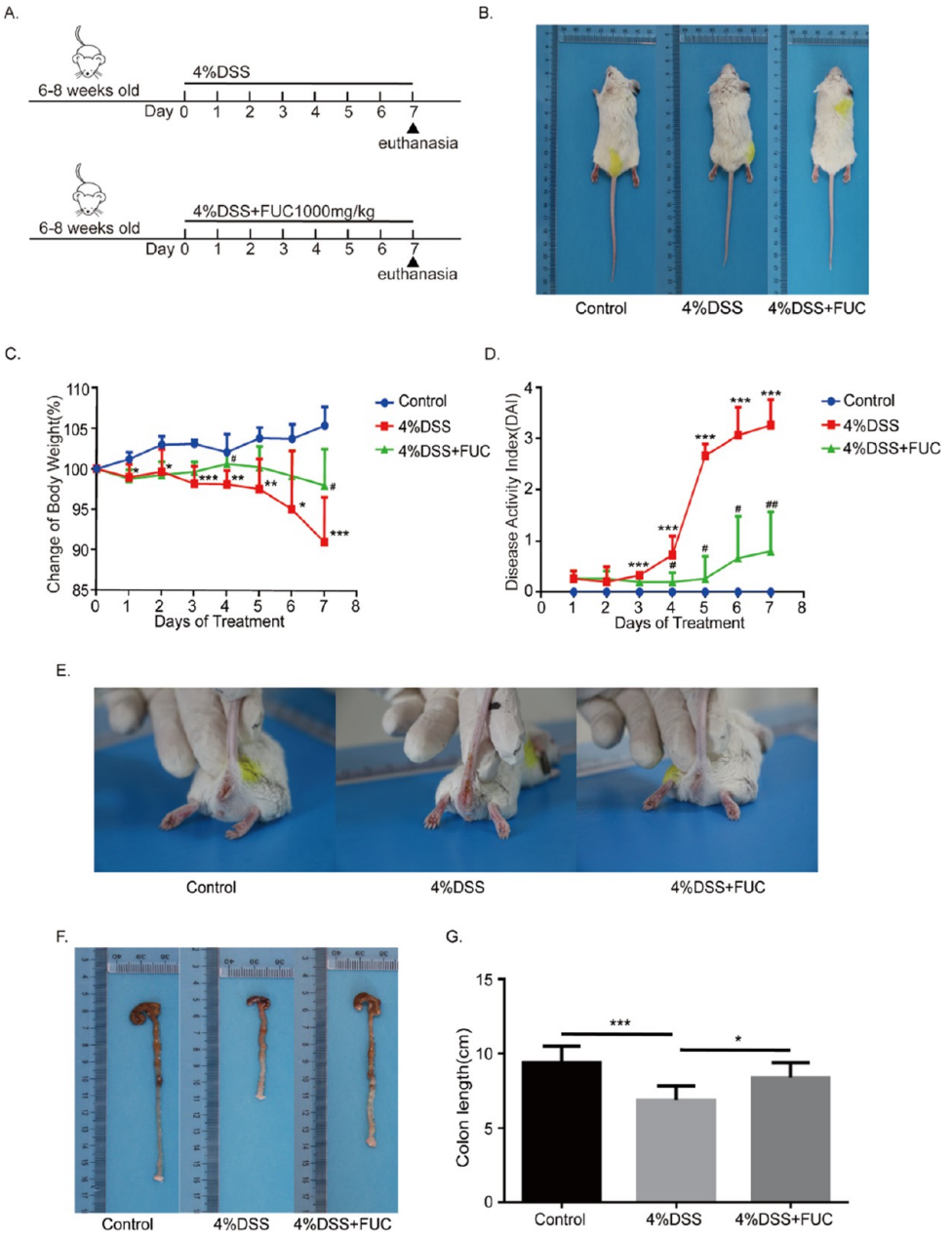

Figure 2. Fucoidan relieves colitis induced by DSS in mice. (A) Diagram of the animal study design. (B) Appearance of mice in the control group, model group, and treatment group, respectively. (C) Weight of mice in the control group, model group, and treatment group, respectively. (D) Evaluation of disease activity index (DAI) of mice in the control group, model group, and treatment group, respectively. (E) Appearance of the anus of mice in the control group, model group, and treatment group, respectively. (F) Pictures of the colorectum of mice in the control group, model group, and treatment group, respectively. (G) Statistical graphs of the colorectal length of mice in the control group, model group, and treatment group, respectively. $^{*}P < 0.05$ vs Control, $^{**}P < 0.01$ vs Control, $^{***}P < 0.001$ vs Control; $^{\#}P < 0.05$ vs 4% DSS, $^{\#\#}P < 0.01$ vs 4% DSS.

min, denaturation at 98 °C for 10 s, annealing at 50 °C for 30 s, and extension at 7 °C for 30 s, with a total of 30 cycles; the final elongation step was carried out at 72 °C for 5 min. The PCR products were mixed and purified for quantification and identification. The sequencing libraries were generated by a TIANSeq Fast DNA Library Prep Kit (Illumina, TIANGEN Biotech, China). The library quality was evaluated on the Qubit@ 2.0 Fluorometer (Thermo Scientific) and Agilent Bioanalyzer 2100 system. Finally, the sequencing of the constructed library was performed on the Illumina platform using the 2 × 250 bp paired-end protocol and data analysis was conducted.

Statistical Analysis. The above experiment was performed at least thrice. The GraphPad Prism7.0 software was used for graphing and statistical analysis. Apoptosis detection was completed using the BD FACS Aria II flow cytometer, and data were analyzed by Treestar Flowjo 10.0 software. Cell cycle detection and data analysis were conducted by a CytExpert 2.3 flow cytometer. All variables were presented as mean ± SD. The Kruskal–Wallis test was used for analyzing microbiological and physiological indicators. Other statistics were performed by Student's *t*-test. The significant statistical difference was accepted at $P < 0.05$.

RESULTS

Cytotoxicity of Fucoidan to FHC. To investigate what kind of cytotoxic effect fucoidan exerts on normal colonic cells, we first treated normal colonic epithelial cells, FHC, with 0, 50, 100, 250, 500, 750, and 1000 $\mu g\ mL^{-1}$ of fucoidan and examined their survival rate after 24, 48, and 72 h of fucoidan treatment by

https://doi.org/10.1021/acs.jafc.2c02357
J. Agric. Food Chem. 2022, 70, 9463−9476

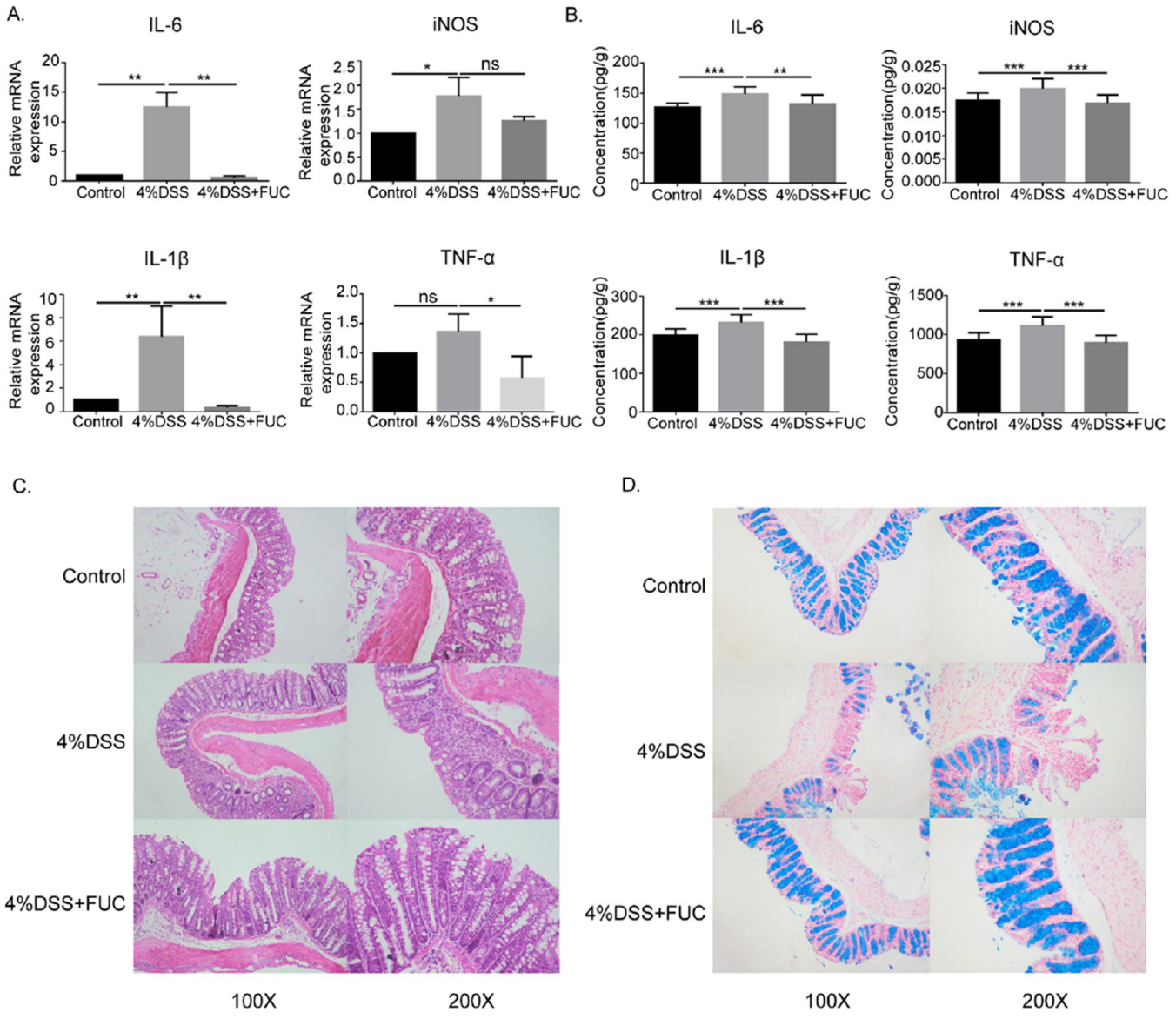

Figure 3. Fucoidan relieves DSS-induced intestinal inflammation and barrier damage in mice. (A) RT-qPCR results of inflammatory factors in colon tissues of mice. (B) Statistical graph of ELISA results of inflammatory factors in colon tissues of mice. (C) HE staining results of mice colon tissue. (D) Results of Alcian blue staining of mouse colon tissue. $^{*}P < 0.05$, $^{**}P < 0.01$, $^{***}P < 0.001$.

MTT proliferation assay. There was no significant difference between the survival rate of the FHC cells treated with different concentrations of fucoidan and those treated without fucoidan at different treatment times (Figure 1A). Hence, it can be suggested that fucoidan did not exert any cytotoxic effect on FHC and it could be used for subsequent experiments.

Fucoidan Relieves LPS-Induced Inflammation of FHC Cells. We used 20 μg mL^{-1} of LPS to induce inflammation in the FHC. Next, the cells were treated with fucoidan at different concentrations. The RT-qPCR results showed that the reexpression levels of IL-8, IL-6, TNF-α, and IL-1β in LPS-stimulated FHC significantly increased. The inflammatory factor expression of FHC administered with 50 μg mL^{-1} of fucoidan showed a downward trend; however, the difference was not statistically significant (Figure 1B). When 100 μg mL^{-1} of fucoidan was used, the expression of inflammatory factors in the FHC cells showed a significant decrease (Figure 1B). Meanwhile, WB results revealed that the p-STAT3 levels and the levels of cellular inflammatory factors, including IL-6, significantly increased in FHC cells under LPS stimulation. However, their expression levels reduced a little after fucoidan intervention (Figure 1C,D). Hence, fucoidan can alleviate the LPS-induced inflammation of FHC cells.

Fucoidan Relieves DSS-Induced Colitis in Mice. Cellular-level studies showed that fucoidan has an anti-inflammatory effect on FHC. This result prompted us to determine whether fucoidan exerts an inhibitory effect on the generation and progression of mice colitis. The treatment process for mice is shown in Figure 2A, in which we also referred to previous modeling approaches and the concentration of DSS used.[30,31] A significant decrease in body weight and the presence of diarrhea and bloody stools in mice were detected when 4% DSS drinking water was used (Figure 2B,C,E). We scored the mice with DAI for weight loss, diarrhea, and feces containing blood. The results demonstrated a significant increase in the scores of mice with colitis (Figure 2D). However, the mice showed some relief from weight loss, diarrhea, and blood in stool with fucoidan intervention (Figure 2B,C,E). At the same time,

https://doi.org/10.1021/acs.jafc.2c02357
J. Agric. Food Chem. 2022, 70, 9463−9476

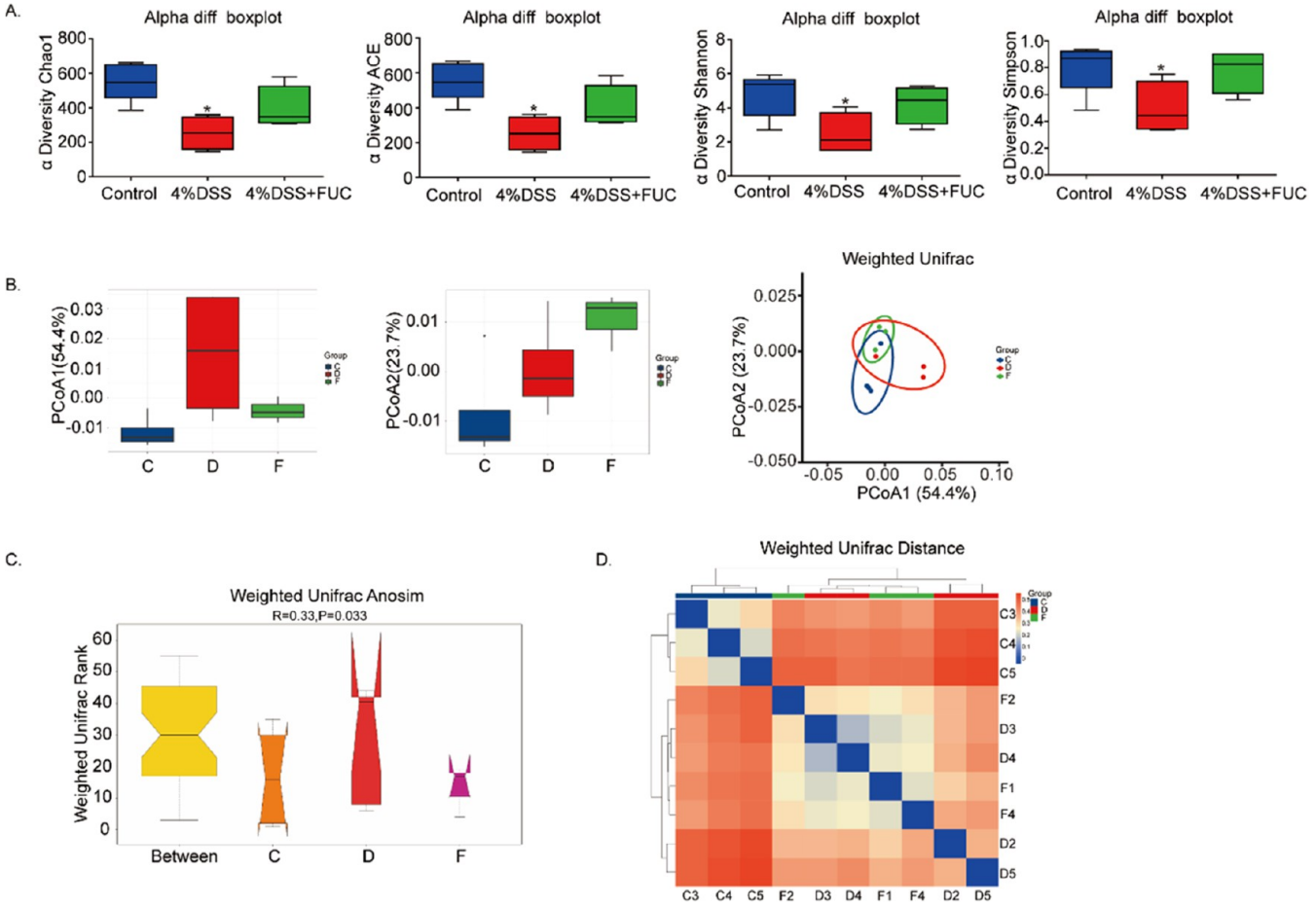

Figure 4. Fucoidan alters the diversity of intestinal microbial composition in mice with colitis. C: Control; D: 4% DSS Model; F: FUC Treatment. (A) α diversity index of the intestinal flora. (B) PCOA analysis. (C) Weighted UniFrac clustering β diversity analysis (Anosim). (D) Cluster analysis of samples. $^{*}P < 0.05$.

DAI scores significantly reduced (Figure 2D). In Figure 2F, we can see that the cecum of the mice with colitis atrophied. We measured the colorectal length from the lower end of the cecum to the anus and found that the colorectal length was significantly reduced in colitis mice (Figure 2G). However, fucoidan intervention normalized the cecum size and restored the colorectal length.

Fucoidan Relieves DSS-Induced Colonic Inflammation and Intestinal Barrier Damage in Mice. To verify the role of fucoidan in affecting the expression of inflammatory factors in the intestinal tissues of mice with colitis, we detected the mRNA levels of inflammatory factors in the colonic tissues of mice in each group. The results are shown in Figure 3A. The daily drinking water containing 4% DSS caused a significant elevation in the relative expression of IL-1β, IL-6, and iNOS mRNA in the colonic tissues of mice. In addition, a rising trend of TNF-α was noted, although no statistical difference was detected. To further explore changes in the protein levels of the abovementioned inflammatory factors, we conducted ELISA experiments. The results were consistent with the gene expression levels. The protein levels of IL-1β, IL-6, TNF-α, and iNOS were significantly higher in the colonic tissues in the colitis model group than that obtained in the control group. The fucoidan intervention can effectively inhibit the expression of protein levels of the abovementioned inflammatory factors (Figure 3B). To further assess the intestinal tissue morphology and intestinal inflammation, we performed the HE staining of colonic tissues. The results are shown in Figure 3C. The structure of the colonic tissue of mice with colitis was significantly damaged, as shown by the abnormal crypt structure, damaged epithelial cells, and inflammatory cell infiltration. However, fucoidan intervention significantly alleviated the damage in mice. Figure 3D shows changes in the intestinal mucus in the mice of different groups. Alcian blue staining showed the formation of a significantly large lesion of the mucus layer in the colon of the mice of the model group. When fucoidan was supplied to these mice, their intestinal mucus layer was maintained in a more normal state.

Fucoidan Changes the Composition of Gut Microbes in Colitis Mice. To assess the change in the intestinal internal flora composition in mice with colitis under fucoidan intervention, we analyzed the cecum content of each group of mice by 16S rDNA sequencing. The results showed that ACE and Chao1 indices, which indicate the abundance of microflora communities, decreased significantly in the mice of the model group. Similarly, Shannon and Simpson indices, which represent the diversity of microbial communities, also decreased significantly in the mice of the model group (Figure 4A). The presence of an inflammatory environment reduced both the diversity and abundance of the microflora environment of the mouse gut. However, the fucoidan intervention reversed this decline. In addition, the β-diversity analysis showed a significant difference in the composition of the mouse gut community among the three groups, with more differences between groups than within groups (Figure 4C). PCOA analysis revealed a

https://doi.org/10.1021/acs.jafc.2c02357
J. Agric. Food Chem. 2022, 70, 9463−9476

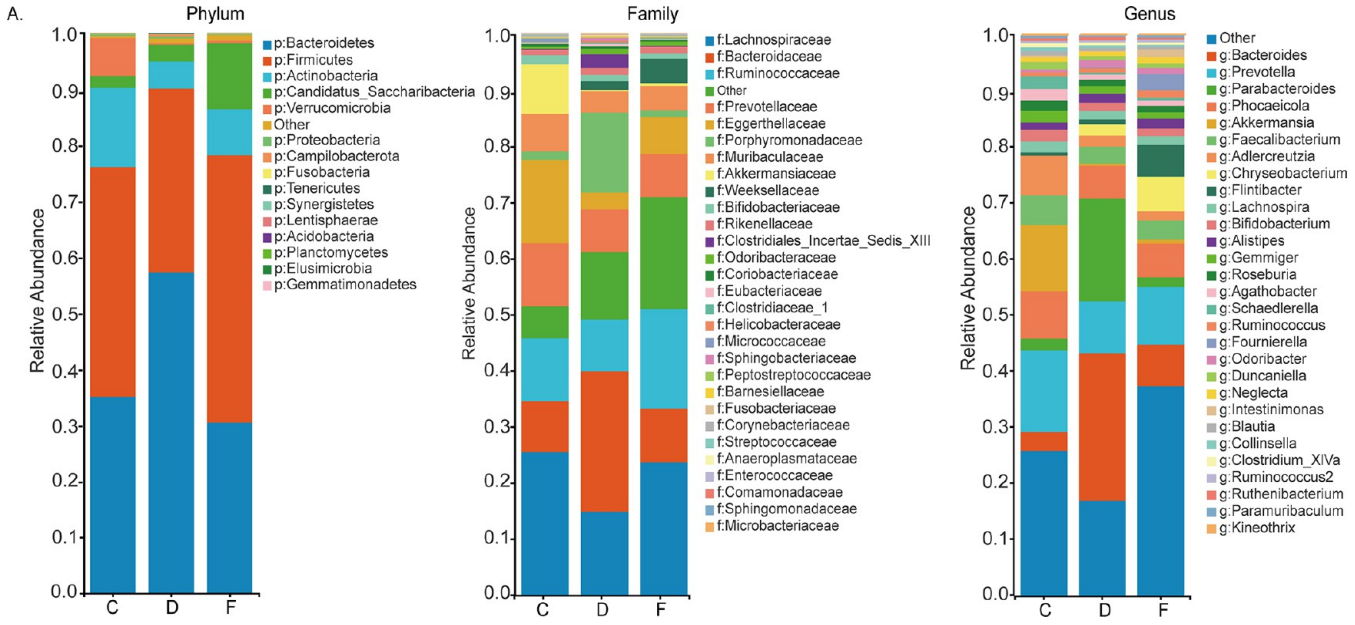

Figure 5. Fucoidan changes the relative abundance composition of the mouse gut induced by DSS. C: Control; D: 4% DSS Model; F: FUC Treatment. Relative abundance composition at the (A) phylum level, (B) family level, and (C) genus level.

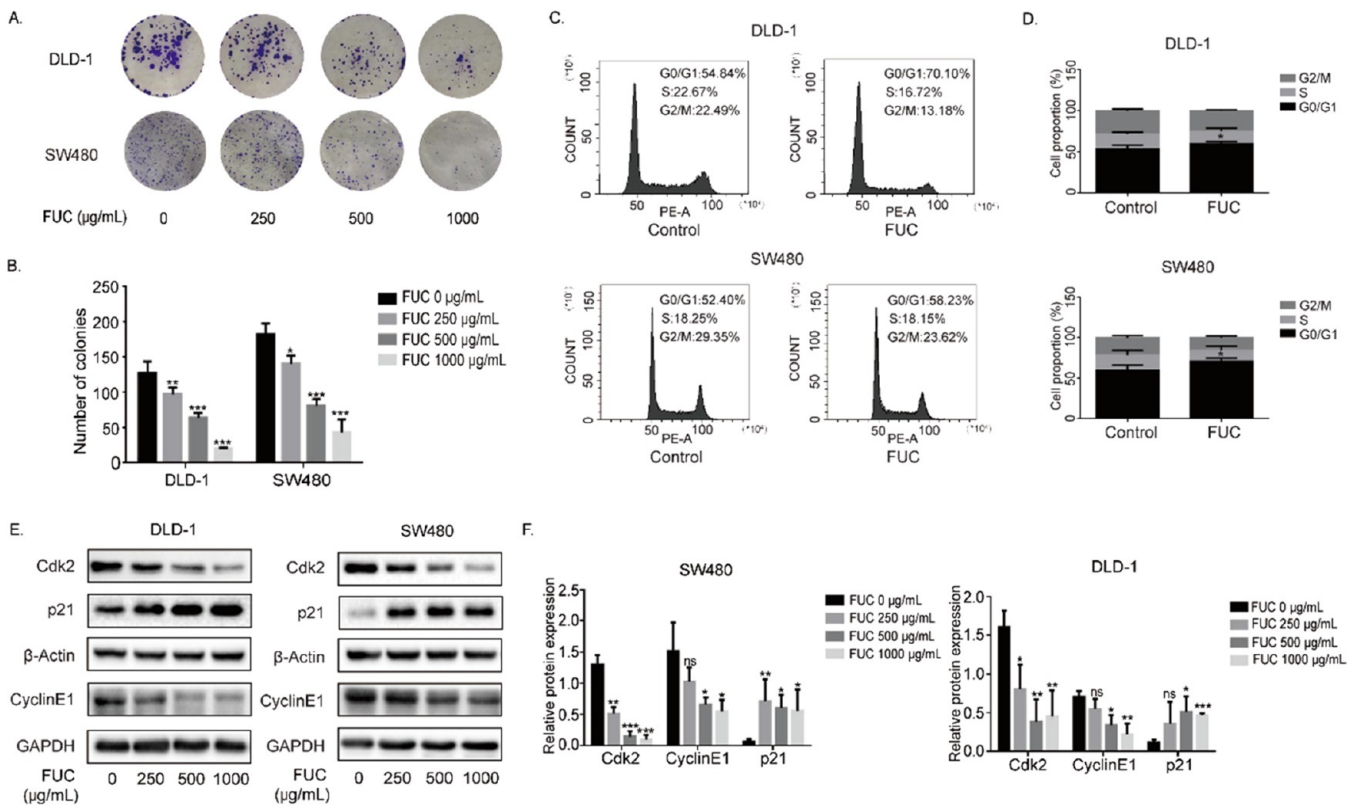

Figure 6. Fucoidan inhibits colony formation and arrests the DLD-1 and SW480 cell cycle. (A) Results of DLD-1 and SW480 colony-formation experiment. (B) Statistical analysis of the colony-formation experiment. (C) Flow cytometry results of DLD-1 and SW480. (D) Statistical analysis of flow cytometry results. (E) Western blot results of DLD-1 and SW480 cycle-related proteins. (F) Statistical analysis of western blot results of DLD-1 and SW480 cycle-related proteins. $^{*}P < 0.05$, $^{**}P < 0.01$, $^{***}P < 0.001$.

difference in the microflora composition of the three groups of mice (Figure 4B). Cluster analysis showed that the control groups were clustered separately from the model and treatment groups, which were clustered together (Figure 4D). Relative abundance composition analysis demonstrated a significant decline in the ratio of Firmicutes/Bacteroidetes in mice of the model group; however, this ratio rebounded in the mice treated with fucoidan (Figure 5). These results suggested that fucoidan may play a role in maintaining the intestinal microecology in mice with colitis.

Fucoidan Inhibits DLD-1 and SW480 Cell Clone Formation and Arrests the Cell Cycle of DLD-1 and

https://doi.org/10.1021/acs.jafc.2c02357
J. Agric. Food Chem. 2022, 70, 9463−9476

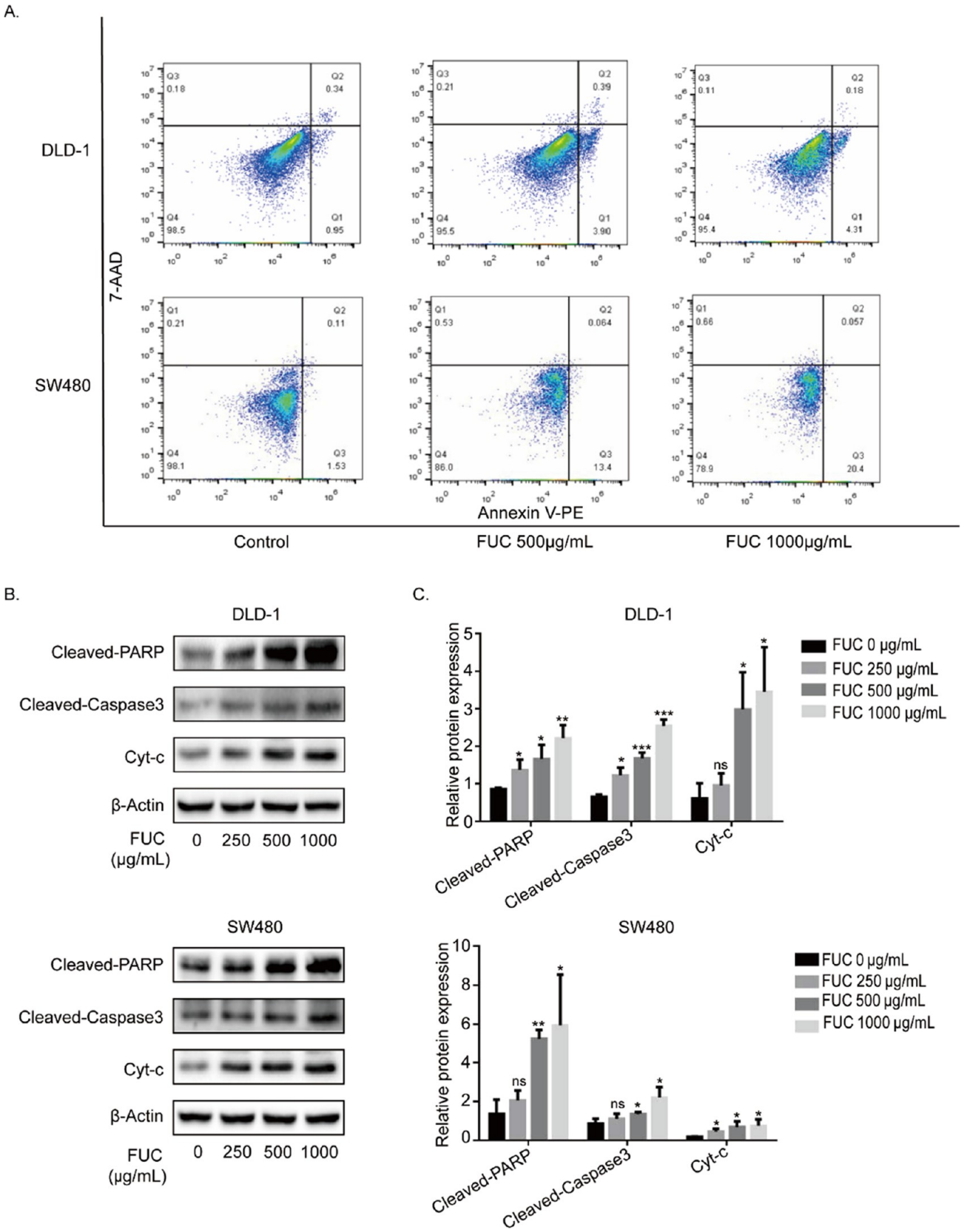

Figure 7. Fucoidan promotes the apoptosis of DLD-1 and SW480 cells. (A) Flow cytometry apoptosis results of DLD-1 and SW480. (B) WB results of DLD-1 and SW480 apoptosis-related proteins. (C) Statistical analysis of WB results of DLD-1 and SW480 apoptosis-related proteins. $^{*}P < 0.05$, $^{**}P < 0.01$, $^{***}P < 0.001$.

SW480. To investigate the effects of fucoidan at different levels on the proliferation capabilities of CRC cells (SW480 and DLD-1), we performed colony-formation experiments. As shown in Figure 6A, the number of colonies formed in the SW480 and

https://doi.org/10.1021/acs.jafc.2c02357
J. Agric. Food Chem. 2022, 70, 9463−9476

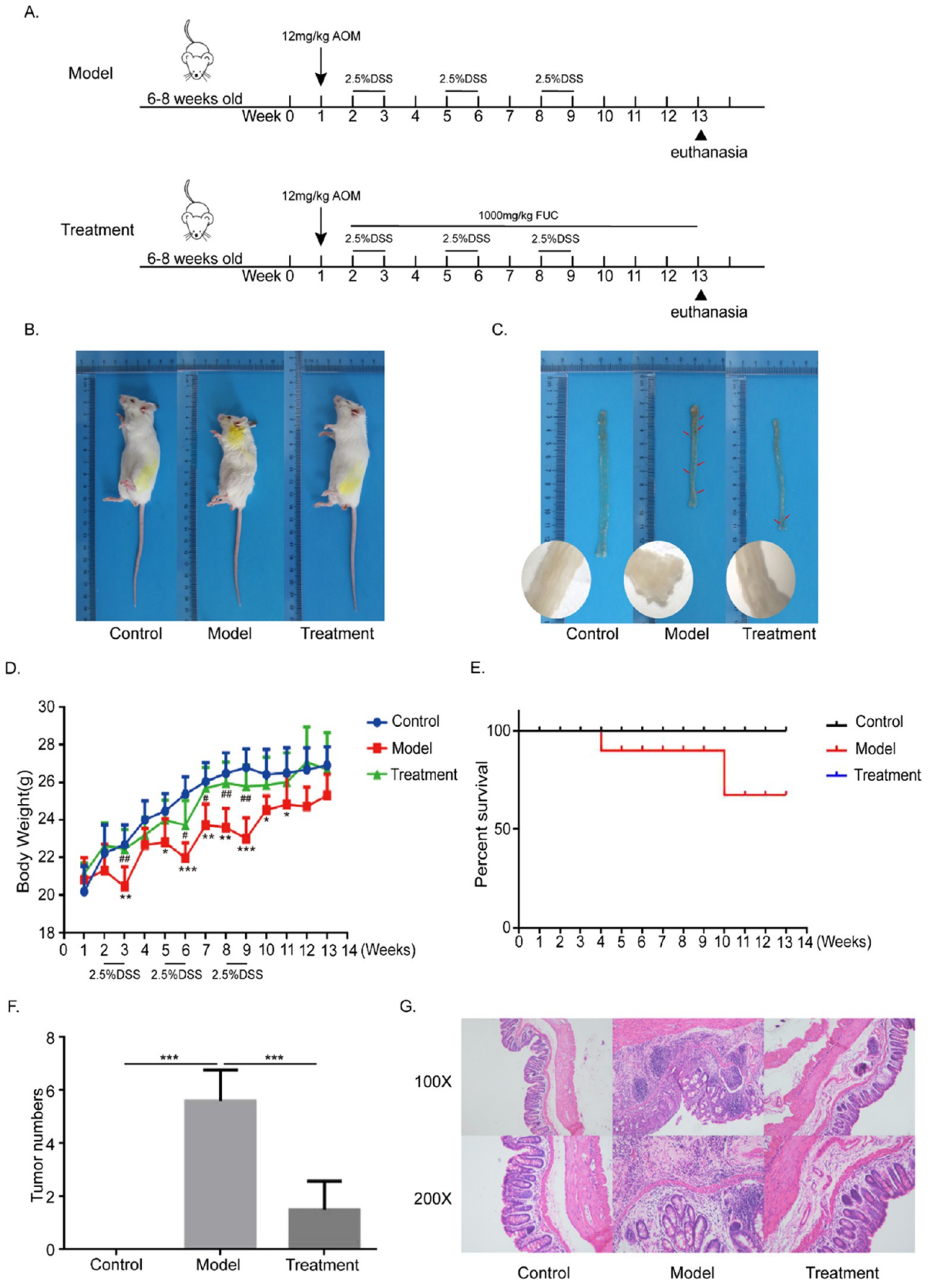

Figure 8. Fucoidan inhibits the occurrence and development of colorectal cancer. (A) Diagram of the animal study design. (B) Appearance of mice in the control group, model group, and treatment group, respectively. (C) Colorectal tissues of mice in the control, model, and treatment groups, respectively. (D) Weight of mice in the control, model, and treatment groups, respectively. (E) Survival curve of the control, model, and treatment groups, respectively. (F) Number of tumors in the mice of the control, model, and treatment groups, respectively. (G) HE staining results of mice rectum tissue. $^{*}P < 0.05$ vs Control, $^{**}P < 0.01$ vs Control, $^{***}P < 0.001$ vs Control; $^{\#}P < 0.05$ vs Model, $^{\#\#}P < 0.01$ vs Model.

https://doi.org/10.1021/acs.jafc.2c02357
J. Agric. Food Chem. 2022, 70, 9463−9476

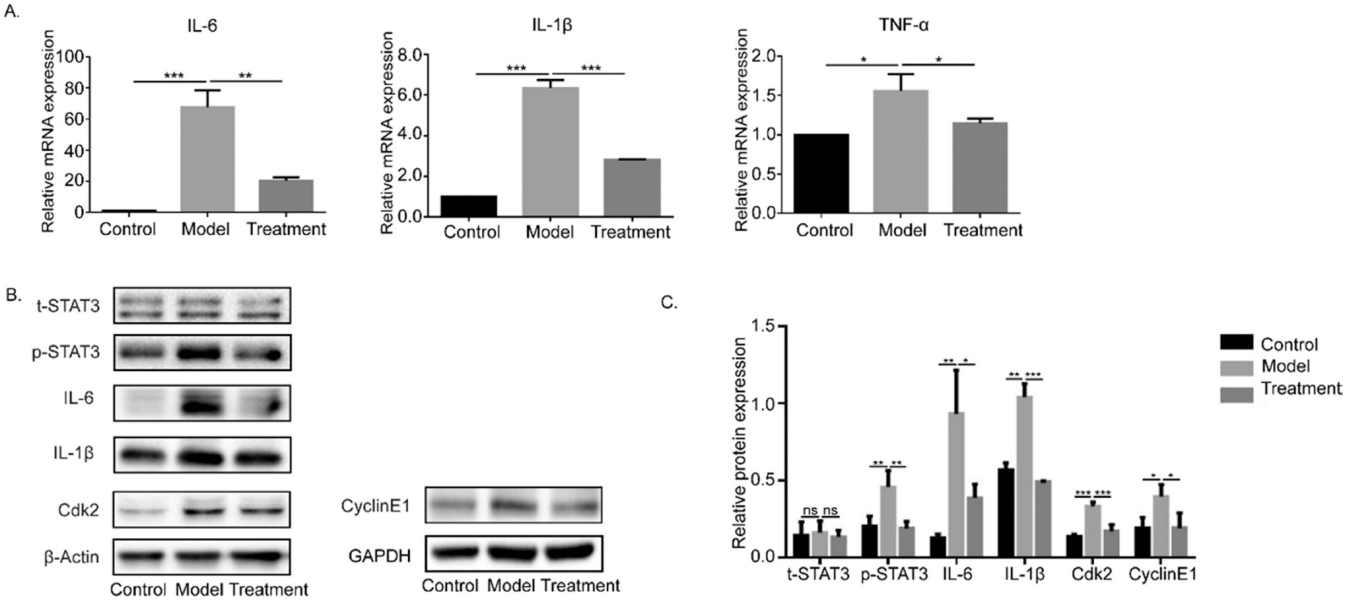

Figure 9. Fucoidan inhibits the occurrence and development of colorectal cancer by inhibiting the expression of cycle-related proteins and inflammation-related proteins. (A) RT-qPCR results of inflammatory factors in mouse rectum tissue. (B) WB results of related proteins in rectal tissue. (C) Statistical analysis of WB results of related proteins in rectal tissue. $^{*}P < 0.05$, $^{**}P < 0.01$, $^{***}P < 0.001$.

DLD-1 cells treated with different levels of fucoidan decreased in a dose-dependent manner (Figure 6B). To further explore the influence of fucoidan on the cell cycle of DLD-1 and SW480-human CRC, fucoidan at a concentration of 250 μg mL^{-1} was used to treat the cells. The results are shown in Figure 6C,D. The DLD-1 and SW480 cells were arrested at the G0/G1 phase by fucoidan. Next, we used western blotting (WB) to measure the expression of related proteins in the signal pathways involved in the cell cycle. Figure 6E,F shows that the expression of Cdk2 and cyclinE1 proteins in DLD-1 and SW480 cells decreased, while that of p21 proteins increased in a dose-dependent manner. Hence, fucoidan can enhance the expression of p21, inhibit that of Cdk2 and cyclinE1, and block the cycle of SW480 and DLD-1.

Fucoidan Promotes Apoptosis of SW480 and DLD-1 Cells. To further explore the influence of fucoidan on CRC cell apoptosis, we used flow cytometry to measure the occurrence of apoptosis at different concentrations of fucoidan. The results showed that fucoidan can promote the apoptosis of both SW480 and DLD-1 cells (Figure 7A). To further study the molecular mechanism through which fucoidan promotes this apoptosis, we detected relevant proteins in the apoptosis pathway by WB. The WB results showed that the proteins related to the apoptosis (cleaved-caspase3, cleaved-PARP, and Cyt-c) of DLD-1 and SW480 cells increased with an increase in the fucoidan concentration (Figure 7B); the difference was statistically significant (Figure 7C). Hence, fucoidan promotes the apoptosis of SW480 and DLD-1 cells.

Fucoidan Inhibits the Occurrence and Development of CRC *In Vivo*. To assess the effect of fucoidan on the inhibition of colorectal tumor formation *in vivo*, we established a CRC mouse model using the classical CRC modeling approach (Figure 8A). At the same time, gavage intervention with fucoidan was performed on the treated group. Figure 8B shows the difference in the appearance of the mice in each group. Compared to the mice in the control group, the mice in the model group were thin and had poorer hair color; however, this poor condition significantly improved in the fucoidan-intervention group. As shown in Figure 8D, the DSS intervention significantly decreased the body weight in the model group mice, while the fucoidan intervention reversed this trend. During the entire experimental period, the model group showed the phenomenon of individual mice death. In addition, the survival rate decreased in the model group, whereas no mice died in the treatment group (Figure 8E). Assessment of tumor formation in the colorectal tissues of mice showed a significant decline in the number of tumors formed in the fucoidan-intervention group (Figure 8C,F). To further confirm the tumor, we performed a histological evaluation of the rectal tissues of mice. The results of HE staining are shown in Figure 8G. The control mice had normal morphology of tissues, while the rectal tissues of the mice in the model group were structurally disorganized with obvious epithelial hyperplasia. Infiltration by a large number of inflammatory cells and lymph node hyperplasia were also visible. In contrast, the tissues under fucoidan intervention showed no significant hyperplasia, and the infiltration of inflammatory cells and lymph node hyperplasia were significantly alleviated. Next, we performed further validation to confirm the expression of the proteins related to the cell cycle and inflammation-related function in the intestinal tissue of mice in each group. The results of RT-qPCR demonstrated that the relative expression of inflammatory factors significantly increased in the mice of the model group, whereas it decreased in the fucoidan-treated mice (Figure 9A). The results of WB revealed that the levels of inflammation-related proteins (p-STAT3, TNF-α, IL-1β, and IL-6) and cycle-related proteins (Cdk2 and cyclinE1) showed an upward trend in the mice of the model group. Compared with the mice in the model group, the expression of these proteins in the mice of the treatment group significantly decreased (Figure 9B,C). Hence, fucoidan plays an essential role in inhibiting inflammation-related tumors.

DISCUSSION

Intestinal inflammation is a key risk factor for the progression of enterocolitis to CRC. In addition, intestinal microbial dysbiosis and impaired intestinal barrier are key to this inflammatory

https://doi.org/10.1021/acs.jafc.2c02357
J. Agric. Food Chem. 2022, 70, 9463−9476

process.[7] Although the causal relationship between microorganisms and their metabolites and intestinal diseases is not yet fully understood,[32] under normal circumstances, intestinal microbes maintain a dynamic balance. Once this balance is upset, an increase in the number of "bad" microbes may exacerbate intestinal inflammation. The presence of an inflammatory environment in the gut may further disrupt the composition of intestinal microflora of mice and promote the progression of inflammation-associated CRC.[33] The presence of an inflammatory environment in the gut may disrupt the gut microbiome in mice.

Although the mechanisms underlying this association are not yet fully understood, repeated cycles of exposure to inflammatory damage and epithelial regeneration may be a contributing factor to gut inflammation. At the tumor-initiation stage, inflammatory cells can produce ROS and reactive nitrogen intermediates, which significantly increase the probability of mutation in neighboring epithelial cells, thereby promoting tumor formation. After the formation of tumors, key transcription factors such as NF-κB and STAT3 can be activated in precancerous cells, which further accelerate the proliferation, growth, and metastasis of cancer cells.[33] The positive effects of fucoidan in relieving intestinal inflammation and improving the intestinal microecology have been reported.[34,35] The noncytotoxic effect of fucoidan on FHC has been confirmed in our study (Figure 1A). Fucoidan also plays a positive role in *in vivo* experiments.[36] It not only reduced LPS-induced inflammation in FHC cells (Figure 1B) but also alleviated the pathological state of colitis mice (Figure 2) and downregulated the expression levels of related inflammatory factors in the intestinal tissue (Figure 3A,B). Furthermore, 16S rDNA sequencing analysis demonstrated that the DSS-induced cecum composition in mice differed from that in normal mice (Figures 4 and 5). This result indicates that fucoidan extracted from *S. fusiforme* can inhibit inflammation and improve the intestinal microecology, both *in vitro* and *in vivo*.

The intestinal mucosal barrier is composed of a chemical barrier, a mechanical barrier, an immune barrier, and a biological barrier, each of which plays an important role in maintaining the normal function of the intestine. The microbial barrier is closely associated with the maintenance of intestinal functions.[37,38] Tight junctions between epithelial cells constitute the mechanical barrier of the intestinal tract and is involved in preventing the translocation of bacteria. Goblet cells mainly secrete mucin. Together with components such as water, inorganic salts, and antibacterial peptides, goblet cells form the intestinal mucus barrier and prevent the infiltration of microorganisms by acting as "filters."[39] Prolonged intestinal inflammation can damage multiple barriers and may result in CRC.[40,41] In this study, we clearly showed through H&E staining that the normal epithelial structure of the colonic tissue of the mice with colitis is destroyed, while the amount of mucin secreted by the goblet cells is significantly reduced under Alcian blue staining (Figure 3C,D). However, mice with colitis after treatment with fucoidan showed a healthier appearance and their weight loss, diarrhea, and other conditions significantly improved. In addition, the histological morphology of the intestinal tissue tended to be normal. Compared with the mice in the control group, those in the treatment group have a more complete mucus barrier and a more stable microbial composition, which is consistent with the reported results.[42,43]

Fucoidan is a polysaccharide with multiple biological functions, including anti-inflammatory and anticancer activities.[44] To further explore these functions and effects of fucoidan, we conducted further studies to investigate its action mechanism in inhibiting the development of inflammation-associated CRC. As a dietary supplement that can prevent and treat diseases, we first demonstrated that fucoidan extracted from *S. fusiforme* has no cytotoxic effect on FHC (Figure 1A). Hence, we conducted related functional tests on CRC cell lines and found that fucoidan had an inhibitory effect on the colony formation of DLD-1 and SW480. We also confirmed that fucoidan can promote cell apoptosis and arrest the cell cycle at the G0/G1 phase (Figure 6C,D). To further explore the molecular mechanisms of its action, we verified the relevant functional proteins through WB. The results demonstrated that fucoidan inhibited the expression levels of proteins related to the cell cycle, including Cdk2 in DLD-1 and SW480, in a concentration-dependent manner (Figure 6E,F), whereas apoptosis-related proteins, cleaved-PARP, cleaved-caspase3, and Cyt-c, increased with an increase in the fucoidan concentration (Figure 7B,C).

Xue et al. used fucoidan extracted from *S. fusiforme* to gavage 1,2-dimethylhydrazine-induced CRC rats and found that the polysaccharide significantly inhibited the formation of colorectal tumors in SD rats.[42] To the best of our knowledge, the inhibition of inflammation-related CRC *in vivo* by fucoidan from *S. fusiforme* has not been investigated yet. Therefore, to further verify the inhibitory effect of fucoidan of *S. fusiforme* origin on the development of CRC *in vivo*, we established a mouse model of CRC and simultaneously intervened with the fucoidan of *S. fusiforme* origin by gavage. The results showed that the intervention of fucoidan significantly alleviated tumor formation in the colorectum of mice (Figure 8). The levels of highly expressed cycle-related proteins in the tissues of mice in the model group also significantly decreased because of the intervention of fucoidan (Figure 9B,C). Thus, it is evident that *S. fusiforme*, a source of fucoidan, can inhibit the developmental process of CRC in mice through cycle-related proteins. In addition, fucoidan, an organic compound with a complex composition, tends to assume diverse cancer inhibitory functions *in vivo*, such as its ability to modulate the immune system, enhance the amount and viability of natural killer cells,[45] and inhibit tumor cell proliferation and angiogenesis,[46] in addition to playing an essential role in the inhibition of metastasis of tumor cells.[47] We also noted an interesting phenomenon. We found that in mouse tissues affected by CRC, the relative expression of the p-STAT3 protein, which mediates inflammation, and the relative mRNA expression of inflammatory factors IL-6, IL-1β, and TNF-α significantly increased in the model mice. The fucoidan intervention resulted in a significant regression of the expression of the abovementioned inflammation-related proteins and inflammatory factors (Figure 9A). The STAT3-mediated pathway is closely associated with the functions of apoptosis and proliferation of cancer cells.[48,49] The evidence from our study is also sufficient to make the following reasonable speculation: fucoidan obtained from *S. fusiforme* may exert a series of tumor-suppressing effects through the STAT3 pathway.

Although the diverse anticancer properties of fucoidan increase its chances of producing increasingly more valuable clinical effects in future trials, it remains somewhat uncertain in light of the current research results. For instance, fucoidan extracted from *Fucus vesiculosus* can arrest the cell cycle of HT29 at the G0/G1 phase by downregulating the protein expression of Cdk4.[50] However, this is different from the arresting of the G0/

https://doi.org/10.1021/acs.jafc.2c02357
J. Agric. Food Chem. 2022, 70, 9463−9476

G1 phase in SW480 and DLD-1 cells, which resulted from the downregulation of the protein expression of Cdk2 by fucoidan. This phenomenon may occur because of the following facts.

(1) The source of our fucoidan is different from that used in other research studies. In addition, *S. fusiforme* of different origins may also have differences in its nutritional components.
(2) There are huge differences in the effective components owing to the use of different extraction processes.
(3) The cells that fucoidan acts on are different.

Therefore, we believe that the mechanism of fucoidan obtained from different sources using different processes on cancer cells may also be different.

In conclusion, we not only clarified the functional mechanism through which fucoidan inhibits CRC *in vitro* but also successfully corroborated it in *in vivo* experiments. This study confirmed that fucoidan extracted from *S. fusiforme* could inhibit the development of CRC through inhibiting the process of colitis, promoting the apoptosis of tumor cells, and blocking the cycle of cancer cells.

AUTHOR INFORMATION

Corresponding Author

Yongliang Lou − *Wenzhou Key Laboratory of Sanitary Microbiology, Key Laboratory of Laboratory Medicine, Ministry of Education, China, School of Laboratory Medicine and Life Sciences, Wenzhou Medical University, Wenzhou 325035 Zhejiang, China; Colorectal Cancer Research Center, Wenzhou Medical University, Wenzhou 325035 Zhejiang, China*; Phone: +86 577 86699652; Email: louyongliang2013@163.com

Authors

Xiang Li − *Wenzhou Key Laboratory of Sanitary Microbiology, Key Laboratory of Laboratory Medicine, Ministry of Education, China, School of Laboratory Medicine and Life Sciences, Wenzhou Medical University, Wenzhou 325035 Zhejiang, China; Colorectal Cancer Research Center, Wenzhou Medical University, Wenzhou 325035 Zhejiang, China;* orcid.org/0000-0001-6346-1574

Shijun Xin − *Wenzhou Key Laboratory of Sanitary Microbiology, Key Laboratory of Laboratory Medicine, Ministry of Education, China, School of Laboratory Medicine and Life Sciences, Wenzhou Medical University, Wenzhou 325035 Zhejiang, China; Colorectal Cancer Research Center, Wenzhou Medical University, Wenzhou 325035 Zhejiang, China*

Xiaoqun Zheng − *Wenzhou Key Laboratory of Sanitary Microbiology, Key Laboratory of Laboratory Medicine, Ministry of Education, China, School of Laboratory Medicine and Life Sciences, Wenzhou Medical University, Wenzhou 325035 Zhejiang, China; Colorectal Cancer Research Center, Wenzhou Medical University, Wenzhou 325035 Zhejiang, China*

Liqin Lou − *Wenzhou Key Laboratory of Sanitary Microbiology, Key Laboratory of Laboratory Medicine, Ministry of Education, China, School of Laboratory Medicine and Life Sciences, Wenzhou Medical University, Wenzhou 325035 Zhejiang, China; Colorectal Cancer Research Center, Wenzhou Medical University, Wenzhou 325035 Zhejiang, China*

Shiqing Ye − *Wenzhou Key Laboratory of Sanitary Microbiology, Key Laboratory of Laboratory Medicine, Ministry of Education, China, School of Laboratory Medicine and Life Sciences, Wenzhou Medical University, Wenzhou 325035 Zhejiang, China; Colorectal Cancer Research Center, Wenzhou Medical University, Wenzhou 325035 Zhejiang, China*

Shengkai Li − *Wenzhou Key Laboratory of Sanitary Microbiology, Key Laboratory of Laboratory Medicine, Ministry of Education, China, School of Laboratory Medicine and Life Sciences, Wenzhou Medical University, Wenzhou 325035 Zhejiang, China; Colorectal Cancer Research Center, Wenzhou Medical University, Wenzhou 325035 Zhejiang, China*

Qilong Wu − *Wenzhou Key Laboratory of Sanitary Microbiology, Key Laboratory of Laboratory Medicine, Ministry of Education, China, School of Laboratory Medicine and Life Sciences, Wenzhou Medical University, Wenzhou 325035 Zhejiang, China; Colorectal Cancer Research Center, Wenzhou Medical University, Wenzhou 325035 Zhejiang, China*

Qingyong Ding − *Wenzhou Key Laboratory of Sanitary Microbiology, Key Laboratory of Laboratory Medicine, Ministry of Education, China, School of Laboratory Medicine and Life Sciences, Wenzhou Medical University, Wenzhou 325035 Zhejiang, China; Colorectal Cancer Research Center, Wenzhou Medical University, Wenzhou 325035 Zhejiang, China*

Ling Ji − *Colorectal Cancer Research Center, Wenzhou Medical University, Wenzhou 325035 Zhejiang, China; The First Affiliated Hospital of Wenzhou Medical University, Wenzhou 325035 Zhejiang, China*

Chunrong Nan − *Wenzhou Key Laboratory of Sanitary Microbiology, Key Laboratory of Laboratory Medicine, Ministry of Education, China, School of Laboratory Medicine and Life Sciences, Wenzhou Medical University, Wenzhou 325035 Zhejiang, China*

Complete contact information is available at: https://pubs.acs.org/10.1021/acs.jafc.2c02357

Author Contributions

[⊥]X.L., S.X., and X.Z. contributed equally to this work. Study concept and design: X.L., Y.L., and L.J. Cell studies: L.J., C.N., S.X., and X.Z. Analysis and interpretation of data: S.X., L.L., S.L., and Q.W. Animal studies: S.X., S.Y., L.L., and Q.D. Manuscript draft: S.X., X.L., and Y.L.

Notes

The authors declare no competing financial interest.
[‖]L.J. and C.N. are equivalent corresponding authors.

ACKNOWLEDGMENTS

This work was supported by the National Science and Technology Major Project (No. 2018ZX10201001-009), the Key Discipline of Zhejiang Province in Medical Technology (First Class, Category A), and the Health Project of the Science and Technology Department of Wenzhou (Nos. Y20180070 and Y2020218).

ABBREVIATIONS

AOM, azoxymethane; BCA, bicinchoninic acid; DAI, disease activity index; CRC, colorectal cancer; DMEM, Dulbecco's Modified Eagle Medium; DMSO, dimethyl sulfoxide; DSS, dextran sulfate sodium; FBS, fetal bovine serum; IBD, inflammatory bowel disease; LEfSe, linear discriminant analysis

effect size; MTT, 3-(4,5-dimethyl-2-thiazolyl)-2,5-diphenyl-2-H-tetrazolium bromide; PCoA, principal coordinates analysis; PCR, polymerase chain reactions; p-STAT3, phosphorylated STAT3; RNI, reactive nitrogen intermediates; ROS, reactive oxygen species; WB, western blot

REFERENCES

(1) Sung, H.; Ferlay, J.; Siegel, R. L.; et al. Global Cancer Statistics 2020: GLOBOCAN Estimates of Incidence and Mortality Worldwide for 36 Cancers in 185 Countries. *CA: Cancer J. Clin.* **2021**, *71*, 209−249.

(2) O'Keefe, S. J. D. Diet, microorganisms and their metabolites, and colon cancer. *Nat. Rev. Gastroenterol. Hepatol.* **2016**, *13*, 691−706.

(3) Percario, R.; Panaccio, P.; di Mola, F. F.; Grottola, T.; Di Sebastiano, P. The Complex Network between Inflammation and Colorectal Cancer: A Systematic Review of the Literature. *Cancers* **2021**, *13*, No. 6237.

(4) Zhao, Z.; Zheng, L.; Chen, W.; et al. Delivery strategies of cancer immunotherapy: recent advances and future perspectives. *J. Hematol. Oncol.* **2019**, *12*, 126.

(5) Cheng, N.; Bai, X.; Shu, Y.; Ahmad, O.; Shen, P. Targeting tumor-associated macrophages as an antitumor strategy. *Biochem. Pharmacol.* **2021**, *183*, No. 114354.

(6) Afrin, S.; Giampieri, F.; Gasparrini, M.; et al. Dietary phytochemicals in colorectal cancer prevention and treatment: A focus on the molecular mechanisms involved. *Biotechnol. Adv.* **2020**, *38*, No. 107322.

(7) Majumder, S.; Shivaji, U. N.; Kasturi, R.; et al. Inflammatory bowel disease-related colorectal cancer: Past, present and future perspectives. *World J. Gastrointest. Oncol.* **2022**, *14*, 547−567.

(8) Stidham, R. W.; Higgins, P. D. R. Colorectal Cancer in Inflammatory Bowel Disease. *Clin. Colon Rectal Surg.* **2018**, *31*, 168−178.

(9) Yalchin, M.; Baker, A.; Graham, T.; Hart, A. Predicting Colorectal Cancer Occurrence in IBD. *Cancers* **2021**, *13*, No. 2908.

(10) Flores, E.; Mbachi, C.; Achebe, I.; et al. Temporal trend in inpatient mortality in inflammatory bowel disease-associated colorectal cancer vs non-inflammatory colorectal cancer: a nationwide retrospective study. *Int. J. Colorectal Dis.* **2021**, *36*, 701−708.

(11) Ni, J.; Shen, T. C.; Chen, E. Z.; et al. A role for bacterial urease in gut dysbiosis and Crohn's disease. *Sci. Transl. Med.* **2017**, *9*, No. eaah6888.

(12) Yu, L.-H. Microbiota dysbiosis and barrier dysfunction in inflammatory bowel disease and colorectal cancers: exploring a common ground hypothesis. *J. Biomed. Sci.* **2018**, *25*, 79.

(13) Lim, E. S.; Wang, D.; Holtz, L. R. The Bacterial Microbiome and Virome Milestones of Infant Development. *Trends Microbiol.* **2016**, *24*, 801−810.

(14) Glassner, K. L.; Abraham, B. P.; Quigley, E. M. M. The microbiome and inflammatory bowel disease. *J. Allergy Clin. Immunol.* **2020**, *145*, 16−27.

(15) Fong, W.; Li, Q.; Yu, J. Gut microbiota modulation: a novel strategy for prevention and treatment of colorectal cancer. *Oncogene* **2020**, *39*, 4925−4943.

(16) Song, M.; Chan, A. T.; Sun, J. Influence of the Gut Microbiome, Diet, and Environment on Risk of Colorectal Cancer. *Gastroenterology* **2020**, *158*, 322−340.

(17) Bennedsen, A. L. B.; Furbo, S.; Bjarnsholt, T.; et al. The gut microbiota can orchestrate the signaling pathways in colorectal cancer. *Apmis* **2022**, *130*, 121−139.

(18) Li, S.; Liu, J.; Zheng, X.; et al. Tumorigenic bacteria in colorectal cancer: mechanisms and treatments. *Cancer Biol. Med.* **2021**, *18*, 147−162.

(19) Stott, K. J.; Phillips, B.; Parry, L.; May, S. Recent advancements in the exploitation of the gut microbiome in the diagnosis and treatment of colorectal cancer. *Biosci. Rep.* **2021**, *41*, No. BSR20204113.

(20) Louis, P.; Hold, G. L.; Flint, H. J. The gut microbiota, bacterial metabolites and colorectal cancer. *Nat. Rev. Microbiol.* **2014**, *12*, 661−672.

(21) Zhang, R.; Zhang, X.; Tang, Y.; Mao, J. Composition, isolation, purification and biological activities of Sargassum fusiforme polysaccharides: A review. *Carbohydr. Polym.* **2020**, *228*, No. 115381.

(22) van Weelden, G.; Bobiński, M.; Okła, K.; et al. Fucoidan Structure and Activity in Relation to Anti-Cancer Mechanisms. *Mar. Drugs* **2019**, *17*, 32.

(23) Kim, E. J.; Park, S. Y.; Lee, J. Y.; Park, J. H. Fucoidan present in brown algae induces apoptosis of human colon cancer cells. *BMC Gastroenterol.* **2010**, *10*, 96.

(24) Kim, I. H.; Kwon, M. J.; Nam, T. J. Differences in cell death and cell cycle following fucoidan treatment in high-density HT-29 colon cancer cells. *Mol. Med. Rep.* **2017**, *15*, 4116−4122.

(25) Bilan, M. I.; Grachev, A. A.; Ustuzhanina, N. E.; et al. A highly regular fraction of a fucoidan from the brown seaweed Fucus distichus L. *Carbohydr. Res.* **2004**, *339*, 511−517.

(26) Adhikari, U.; Mateu, C. G.; Chattopadhyay, K.; et al. Structure and antiviral activity of sulfated fucans from Stoechospermum marginatum. *Phytochemistry* **2006**, *67*, 2474−2482.

(27) Haroun-Bouhedja, F.; Ellouali, M.; Sinquin, C.; Boisson-Vidal, C. Relationship between sulfate groups and biological activities of fucans. *Thromb. Res.* **2000**, *100*, 453−459.

(28) Palanisamy, S.; Vinosha, M.; Marudhupandi, T.; Rajasekar, P.; Prabhu, N. M. Isolation of fucoidan from Sargassum polycystum brown algae: Structural characterization, in vitro antioxidant and anticancer activity. *Int. J. Biol. Macromol.* **2017**, *102*, 405−412.

(29) Ito, R.; Shin-Ya, M.; Kishida, T.; et al. Interferon-gamma is causatively involved in experimental inflammatory bowel disease in mice. *Clin. Exp. Immunol.* **2006**, *146*, 330−338.

(30) Lee, C.; Hong, S. N.; Kim, Y. H. A glycolipid adjuvant, 7DW8-5, provides a protective effect against colonic inflammation in mice by the recruitment of CD1d-restricted natural killer T cells. *Intest. Res.* **2020**, *18*, 402−411.

(31) Koh, S. J.; Choi, Y. I.; Kim, Y.; et al. Walnut phenolic extract inhibits nuclear factor kappaB signaling in intestinal epithelial cells, and ameliorates experimental colitis and colitis-associated colon cancer in mice. *Eur. J. Nutr.* **2019**, *58*, 1603−1613.

(32) Fobofou, S. A.; Savidge, T. Microbial metabolites: cause or consequence in gastrointestinal disease? *Am. J. Physiol.: Gastrointest. Liver Physiol.* **2022**, *322*, G535−G552.

(33) Abdulla, M. H.; Agarwal, D.; Singh, J.; et al. Association of the microbiome with colorectal cancer development (Review). *Int. J. Oncol.* **2021**, *58*, No. 17.

(34) Lean, Q. Y.; Eri, R. D.; Fitton, J. H.; Patel, R. P.; Gueven, N. Fucoidan Extracts Ameliorate Acute Colitis. *PLoS One* **2015**, *10*, No. e0128453.

(35) O'Shea, C. J.; et al. The effect of algal polysaccharides laminarin and fucoidan on colonic pathology, cytokine gene expression and Enterobacteriaceae in a dextran sodium sulfate-challenged porcine model. *J. Nutr. Sci.* **2016**, *5*, No. e15.

(36) Vigors, S.; O'Doherty, J.; Rattigan, R.; Sweeney, T. Effect of Supplementing Seaweed Extracts to Pigs until d35 Post-Weaning on Performance and Aspects of Intestinal Health. *Mar. Drugs* **2021**, *19*, 183.

(37) Thursby, E.; Juge, N. Introduction to the human gut microbiota. *Biochem. J.* **2017**, *474*, 1823−1836.

(38) Dong, S.; Zhu, M.; Wang, K.; et al. Dihydromyricetin improves DSS-induced colitis in mice via modulation of fecal-bacteria-related bile acid metabolism. *Pharmacol. Res.* **2021**, *171*, No. 105767.

(39) McCauley, H. A.; Guasch, G. Three cheers for the goblet cell: maintaining homeostasis in mucosal epithelia. *Trends Mol. Med.* **2015**, *21*, 492−503.

(40) Bouma, G.; Strober, W. The immunological and genetic basis of inflammatory bowel disease. *Nat. Rev. Immunol.* **2003**, *3*, 521−533.

(41) Cheng, Y.; Ling, Z.; Li, L. The Intestinal Microbiota and Colorectal Cancer. *Front. Immunol.* **2020**, *11*, No. 615056.

(42) Xue, M.; Liang, H.; Ji, X.; et al. Effects of fucoidan on gut flora and tumor prevention in 1,2-dimethylhydrazine-induced colorectal carcinogenesis. *J. Nutr. Biochem.* **2020**, *82*, No. 108396.

https://doi.org/10.1021/acs.jafc.2c02357
J. Agric. Food Chem. 2022, 70, 9463−9476

(43) Xue, M.; Ge, Y.; Zhang, J.; et al. Anticancer properties and mechanisms of fucoidan on mouse breast cancer in vitro and in vivo. *PLoS One* **2012**, *7*, No. e43483.
(44) Besednova, N. N.; Zaporozhets, T. S.; Kuznetsova, T. A.; et al. Extracts and Marine Algae Polysaccharides in Therapy and Prevention of Inflammatory Diseases of the Intestine. *Mar. Drugs* **2020**, *18*, 289.
(45) Zhang, W.; An, E. K.; Park, H. B.; et al. Ecklonia cava fucoidan has potential to stimulate natural killer cells in vivo. *Int. J. Biol. Macromol.* **2021**, *185*, 111−121.
(46) Chen, X.; Sun, L.; Wei, X.; et al. Antitumor effect and molecular mechanism of fucoidan in NSCLC. *BMC Complement. Med. Ther.* **2021**, *21*, 25.
(47) Pan, T. J.; Li, L. X.; Zhang, J. W.; et al. Antimetastatic Effect of Fucoidan-Sargassum against Liver Cancer Cell Invadopodia Formation via Targeting Integrin $\alpha V\beta 3$ and Mediating $\alpha V\beta 3$/Src/E2F1 Signaling. *J. Cancer* **2019**, *10*, 4777−4792.
(48) Fathi, N.; Rashidi, G.; Khodadadi, A.; Shahi, S.; Sharifi, S. STAT3 and apoptosis challenges in cancer. *Int. J. Biol. Macromol.* **2018**, *117*, 993−1001.
(49) Lin, Y.; He, Z.; Ye, J.; et al. Progress in Understanding the IL-6/STAT3 Pathway in Colorectal Cancer. *Onco Targets Ther.* **2020**, *13*, 13023−13032.
(50) Han, Y. S.; Lee, J. H.; Lee, S. H. Fucoidan inhibits the migration and proliferation of HT-29 human colon cancer cells via the phosphoinositide-3 kinase/Akt/mechanistic target of rapamycin pathways. *Mol. Med. Rep.* **2015**, *12*, 3446−3452.

https://doi.org/10.1021/acs.jafc.2c02357
J. Agric. Food Chem. 2022, 70, 9463−9476